

Topological entropy of a stiff ring polymer and its connection to DNA knots

Miyuki K. SHIMAMURA and Tetsuo DEGUCHI

Department of Physics, Faculty of Science
and Graduate School of Humanities and Sciences,
Ochanomizu University
2-1-1 Ohtsuka, Bunkyo-ku, Tokyo 112-8610, Japan

E-mail: miyuki@degway.phys.ocha.ac.jp

Abstract

We discuss the entropy of a circular polymer under a topological constraint. We call it the *topological entropy* of the polymer, in short. A ring polymer does not change its topology (knot type) under any thermal fluctuations. Through numerical simulations using some knot invariants, we show that the topological entropy of a stiff ring polymer with a fixed knot is described by a scaling formula as a function of the thickness and length of the circular chain. The result is consistent with the viewpoint that for stiff polymers such as DNAs, the length and diameter of the chains should play a central role in their statistical and dynamical properties. Furthermore, we show that the new formula extends a known theoretical formula for DNA knots.

keyword topological entropy, circular polymers, random knotting, self-avoiding polygons, knot invariants, DNA knots

1 Introduction

In the last fifteen years, various knotted ring-polymers are synthesized and observed in experiments of chemistry and biology. [1, 2, 3] Once a ring polymer is formed, its topological state, which is given by a knot, is unique and invariant. One of unsolved problems in statistical physics of macromolecules is how to formulate the topological constraint on ring polymers theoretically so that we can investigate topological effects on their statistical and dynamical properties. This problem was addressed by Delbrück in the 60's [4, 5]. Since then, several numerical simulations have been performed [6, 7, 8, 9, 10, 11, 12, 13, 14, 15, 16, 17]. The topological constraint on a ring-polymer is nontrivial. It may severely restrict the available degrees of freedom in the configuration space, and then lead to a large reduction on its entropy.

Let us formulate the topological problem, explicitly. We consider a ring polymer in good solution, whose degree of polymerization corresponds to N units of the Kuhn statistical length [18]. Then, a spatial configuration of the ring polymer can be approximated by a self-avoiding polygon with N

polygonal nodes (or N bonds, N vertices). Here, the length of polygonal segments is given by the Kuhn length.

Let us assume the number $W_K(N)$ of all possible N -noded self-avoiding polygons with a knot K . Then, the topological entropy $S_K(N)$ for the knot K is given by $S_K(N) = k_B \log W_K(N)$. Here k_B is the Boltzmann constant. We remark that the entropy $S(N)$ without any topological constraint is given by $S(N) = k_B \log W(N)$, where $W(N)$ is the number of all self-avoiding polygons with N nodes: $W(N) = \sum_K W_K(N)$. Let us introduce the knotting probability $P_K(N)$ of a knot K . We define it by the probability that a given configuration of a self-avoiding polygon with N nodes is equivalent to the knot K . It is clear that the knotting probability is given by $P_K(N) = W_K(N)/W(N)$. Thus, the decrease of the entropy of the ring polymer due to the topological constraint that it should keep its knot type K is expressed in terms of the knotting probability for the knot K :

$$\begin{aligned} S(N) - S_K(N) &= k_B \log W(N) - k_B \log W_K(N) \\ &= k_B \log(1/P_K(N)). \end{aligned} \quad (1.1)$$

Recently, randomly knotted DNA rings are syn-

thesized in experiments, and the fractions of some knotted species are measured through the electrophoretic separation. [19, 20] Here we remark that the fraction of DNAs with a knot K corresponds to the knotting probability of the knot K . The measurement of the fractions of knotted DNAs is particularly interesting because it gives an excellent method for determining the effective diameter of DNAs, which are negatively charged and surrounded by the clouds of counter ions. The effective diameter of DNAs in an electrolyte solution depends strongly on the concentration of the counter ions. However, it is nontrivial to calculate the effective diameter of DNAs by taking into account the electric double layers around the cylindrical segments. [21, 22] Furthermore, DNA chains are rather stiff; the persistent length (i.e., the Kuhn statistical length) of DNA chains is given by $50 \sim 100$ nm, depending on the ionic concentrations [23], which is much larger than that of polystylenes. [18]

Thermodynamical properties of DNA chains in electrolyte solutions are studied by introducing some models of cylindrical self-avoiding walks. For DNA rings, we introduce a model of self-avoiding polygons consisting of N cylindrical segments with cylindrical radius r where their length is given by the Kuhn length b . Then, let us consider the probability $P_{knotted}(N, r)$ of a cylindrical polygon being knotted (i.e., being a non-trivial knot). For the algorithms of cylindrical self-avoiding polygons [9, 11], it was studied through simulations how the probability $P_{knotted}(N, r)$ should depend on the radius r . The numerical results were analyzed by assuming an exponential dependence in the following:

$$P_{knotted}(N, r) = P_{knotted}(N, 0) \exp\left(-\gamma \frac{r}{b}\right). \quad (1.2)$$

Here γ is a constant to be determined by the simulations. Thus, by measuring the fraction of knotted DNAs and applying the theoretical formula (1.2) to them, the effective diameters of DNA rings in some electrolyte solutions are determined. [19, 20]

In this paper, we introduce a theoretical formula describing the knotting probability of a given knot for stiff ring polymers such as circular DNAs. It describes how the knotting probability depends on the length and radius of the ring polymers. We formulate an algorithm of self-avoiding polygons consisting of cylindrical segments with radius r and unit length. [24] The algorithm is based on the dimerization algorithm, and we call the algorithm the cylindrical ring-dimerization method, or the dimerization method, for short. The method should be useful for studying stiff ring polymers. In fact, it is closely related to the wormlike chain model for polyelectrolytes in electrolyte solutions. [23] Through numerical simulations with the method, we evaluate the knotting probabilities for the cylindrical self-avoiding polygons with several different numbers N of polygonal nodes and different values of

the cylindrical radius r . Then, we show that the new formula gives good fitting curves to the estimates of the knotting probabilities. In fact, the fitting curves fit to the data for the cylindrical polygons of very small as well as very large (even asymptotically large) numbers N of nodes, and of all the different values of the radius r . Furthermore, we show that it extends the known formula (1.2) for the DNA knots. Finally, we discuss some consequences of the theoretical formula of the knotting probability, which may be useful for future study of knotted circular DNAs.

The model of cylindrical self-avoiding polygons should be valid for any real ring polymer in good solution. According to the standard two-parameter theory of polymers, it is expected that any statistical property of polymers can be described by the length and thickness of the chains. [18] The radius of cylindrical segments corresponds to the thickness of ring polymers, which expresses the excluded-volume effect. In appendix A, some algorithms of the cylindrical self-avoiding polygons are shown.

The paper is organized as follows: In §2 we explain the cylindrical ring-dimerization method of our numerical experiment of random knotting. In §3, employing the algorithm discussed in §2, we produce a large number of self-avoiding polygons consisting of cylinders, and present numerical estimates of the knotting probabilities of several different knots such as the trivial knot, non-trivial prime knots ($3_1, 4_1, 5_1, 5_2$), and nontrivial composite knots ($3_1 \# 3_1, 3_1 \# 3_1 \# 3_1$). Then, we find that they are well described by the new theoretical formula of the knotting probability of the cylindrical self-avoiding polygons constructed by the cylindrical ring-dimerization method. In §4, we show that the new formula generalizes the known formula (1.2). Finally, we give some concluding remarks in §5.

2 Methods of Numerical Simulations

2.1 Overview of the numerical experiment of random knotting

We first discuss the outline of our numerical experiment. The knotting probability is evaluated by the following processes: (1) We construct a large number, say M , of self-avoiding polygons of N cylindrical segments with radius r and unit length; (2) Projecting the three-dimensional configurations of the self-avoiding polygons onto a plane, we make their knot diagrams; (3) Calculating some knot invariants for the knot diagrams, we enumerate the number M_K of such polygons that have the same set of values of the knot invariants with a knot K .

For a given number N of polygonal nodes, we produce M polygons with the algorithm of the dimer-

ization method of self-avoiding polygons. In this paper, we set $M = 10^4$. We recall that M_K denotes the number of such polygons that have the same set of values of the knot invariants with the knot K . Then, it is clear that the knotting probability $P_K(N)$ is given by the following

$$P_K(N) = \frac{M_K}{M} \quad (2.1)$$

We note that the algorithm of the dimerization method will be explained in §2.3 and §2.4 (See also §A.1).

2.2 Knot invariants for detecting knot types

In the numerical simulations of the paper, the tool for detecting the knot type of a given polygon is a set of two knot invariants in the following: the determinant $\Delta_K(-1)$ of knot and the Vassiliev-type invariant $v_2(K)$ of the second degree. The values of the invariants for some typical knots are given in Table 1. It is remarked that the two knot invariants have definite advantages for practical purposes. In fact, there exist some algorithms by which we can calculate the two knot invariants in polynomial time with respect to the number of crossing points of a given knot diagram. [25, 26]

2.3 Cylindrical ring-dimerization method

Let us discuss the method [24] for constructing self-avoiding polygons consisting of cylinders with radius r of unit length. It is based on the dimerization algorithm. [27] We recall that it is called the cylindrical ring-dimerization method, or the dimerization method, for short. The method consists of the following processes: (1) We generate a set of chains with cylindrical segments by the dimerization algorithm; (2) We construct polygons by connecting two cylindrical self-avoiding chains with the method of Ref. [10], where we also calculate the statistical weight related to the probability of successful concatenation.

Let us explain the dimerization algorithms for self-avoiding walks, and then for self-avoiding polygons. Under the dimerization algorithm [27], we make a chain by connecting two given subchains if they have no “overlap”; if they have an “overlap”, then we throw away both of the two subchains and we take a new pair of subchains to try. In the method [10] for making self-avoiding polygons, first we pick up a compatible pair of self-avoiding walks, and then we check whether they have any “overlap” or not. If not, we make a new ring by connecting the ends of the two chains; if there is an “overlap”, then we throw them away and take a new pair of

chains. In the concatenating method, we also calculate the statistical weight related to the probability of successful concatenation.

One of the key points of our algorithm is the condition when given two cylindrical segments have an “overlap”. We define the condition of “overlap” between a given pair of segments as follows. First, there is no “overlap” between any pair of adjacent segments, i.e., we neglect the thickness of segments for any pair of adjacent cylindrical segments. Thus, there is no constraint between any next-neighboring segments in our model of cylindrical self-avoiding polygons. Second, two segments have no “overlap” if the minimum distance between the central line segments of cylinders for any given pair of unadjacent cylinders is larger than the diameter $2r$ of cylinders. Here, we have defined the central line segment of a cylinder by the line segment between the centers of the upper and lower disks of the cylinder. For an illustration, we give in Appendix B the algorithm for checking whether any given two cylindrical segments have an “overlap” or not.

The cylinder condition is important in practical applications. We recall that DNA chain as a polyelectrolyte in an electrolyte solution can be modeled by the model of cylindrical self-avoiding polygons since the negatively charged DNA segments with counter ions shielded around them can be approximated effectively as impermeable cylinders of the Kuhn statistical length with the radius given by the Debye screening length.

2.4 Some details of the dimerization algorithm

Let us describe the algorithm of dimerization, more precisely. [27] First, we construct a very large number, say M_0 , of short self-avoiding chains with N_0 cylindrical segments, randomly by a direct method. Then, we pick up a pair of short chains out of the M_0 generated chains randomly, and see whether there is any overlap or not between the chains; we investigate all unadjacent pairs of cylindrical segments of the chains. If there is an overlap, then we give up the chains and consider a new pair of short chains from the beginning. If there is no overlap, then we make a longer chain with length $2N_0$ by connecting the end of one chain to the head of another one. After constructing $M_0/2$ chains with length $2N_0$ by the method, we repeat this construction for the $M_0/2$ longer chains. The scheme of the dimerization algorithm is shown in Fig. 3, which is given by a binary tree. Thus, we can construct very long self-avoiding polygons with the cylinder radius r , quite efficiently. In appendix A, we explain all the detail of the algorithm of the cylindrical ring-dimerization, explicitly.

3 Knotting Probability and Its Fitting Formula

3.1 A brief review on knotting probabilities of ring polymers

We discuss some important known results on the statistics of random knots obtained by numerical simulations with algebraic invariants of knots. In particular, we consider how the knotting probability should depend on the length N of ring polymers.

Let us first consider the knotting probability of the trivial knot. We recall that it is the probability of forming a trivial knot in a given random polygon (or self-avoiding polygon) with N nodes. We denote it by $P_0(N, r)$, and call it the unknotting probability or knotting probability of the trivial knot (or unknot). Here, the symbol $K = 0$ denotes that the knot K is trivial. We also note that the probability $P_{knotted}(N, r)$ of a polygon being knotted is given by the unknotting probability $P_0(N, r)$ as in the following: $P_{knotted}(N, r) = 1 - P_0(N, r)$. Here we recall that if a polygon is equivalent to a nontrivial knot, then we regard it as knotted.

The unknotting probability has been evaluated for different models and methods: some models of the closed random polygons [6, 7, 8], the hedge-hog method [11], and the rod-bead model [10, 13]. For some models of random polygons or self-avoiding polygons, it has been found in Ref. [8, 13] that the unknotting probability has a decreasing exponential dependence on the number N of nodes:

$$P_0(N) = C_0 \exp(-N/N_0). \quad (3.1)$$

Here, the two parameters N_0 and C_0 are to be determined so that eq. (3.1) gives the best fitting curve to the numerical estimates of the unknotting probabilities for different numbers N . We call the parameter N_0 the characteristic length of random knotting of unknot.

Let us consider the case of nontrivial knots. We recall that the knotting probability of a nontrivial knot K is given by the probability $P_K(N)$ of observing the knot K in a given random polygon (or self-avoiding polygon) with N nodes. Knotting probabilities of several nontrivial knots have been evaluated for some different models of random polygons or self-avoiding polygons. [6, 11, 14, 15, 16] Through the simulations with the Vassiliev-type knot invariants [14, 16], it has been found that, for the Gaussian random polygons and the rod-bead self-avoiding polygons, the probabilities of nontrivial knots versus the number N of nodes are well approximated by the fitting curves given by the following formula:

$$P_K(N) = C_K (N/N_K)^{m_K} \exp(-N/N_K). \quad (3.2)$$

Here C_K , N_K and m_K are fitting parameters to be determined from the estimates of the knotting

probabilities obtained numerically. For a given knot K , we call m_K the exponent of the knot. We also call N_K the characteristic length of the knot K .

There are some universal properties of the fitting parameters N_K and m_K of the formula (3.2). For any one of the models investigated, it is found that the values of the parameters N_K are almost the same for any knot K : $N_K \simeq N_0$. [14, 16] Furthermore, it is observed that the parameter m_K of a knot K should be universal for the different models, while the fitting parameters C_K and N_K are model-dependent. [16] Thus, we may consider that the parameter m_K should play a similar role with the critical exponents of critical phenomena. In fact, the formula (3.2) of knotting probability is quite consistent with the asymptotic scaling behaviors of the number $W(N)$ of all the configurations of self-avoiding polygons:

$$W(N) \simeq C\mu^N N^{\alpha-2}, \quad \text{for } N \gg 1. \quad (3.3)$$

Here μ is the growth constant and α corresponds to the critical exponent related to the energy of the n -vector model through the limit of sending n to 0. [28] We can also expect a similar asymptotic expansion for the number $W_K(N)$ of a knot K . Thus, we may call eq. (3.2) a scaling formula of the knotting probability for the knot type K .

Let us now consider effects of excluded volume on the knotting probability. Through the numerical simulations of the cylindrical self-avoiding polygons, it has been found that the excluded-volume parameter such as the cylinder radius plays a central role in the probability of knot formation. [9, 11]. Here, we recall that the probability $P_{knotted}(N, r)$ of a cylindrical self-avoiding polygon being a nontrivial knot depends on the number N of polygonal nodes, the cylindrical radius r , and the Kuhn statistical length b . It was discussed that the probability $P_{knotted}(N, r)$ should depend on the radius r through the exponential factor $\exp(-\gamma r/b)$ such as shown in eq. (1.2), where γ is the proportionality constant determined from the simulations. [9, 11].

The empirical formula (1.2) has been fundamental in the study of random knotting of small circular DNAs. [19, 20] However, it is not valid when N is large enough, as we shall see in §4.3. Here, we recall that N is the number of nodes of cylindrical self-avoiding polygons. Furthermore, we show in §4.4 that our generalized scaling-type formula for the knotting probability of the cylindrical self-avoiding polygons generalizes the formula (1.2).

3.2 Generalized scaling formula for knotting probability of ring polymers

Let us discuss the knotting probability $P_K(N, r)$ of the model of cylindrical self-avoiding polygons con-

constructed by the dimerization method that depends not only on the number N of nodes but also on the cylinder radius r . Generalizing the scaling formula (3.2) which explains only the N -dependence, we introduce the following formula for the probability $P_K(N, r)$:

$$P_K(N, r) = C_K(r) (N/N_K(r))^{m_K(r)} \exp(-N/N_K(r)). \quad (3.4)$$

Here $C_K(r)$, $m_K(r)$, $N_K(r)$ are fitting parameters. As we shall see later in this section, eq. (3.4) gives good fitting curves to numerical estimates of the knotting probability of the cylindrical self-avoiding polygons constructed by the dimerization method.

The formula (3.4) also generalizes another formula of the knotting probability. In a previous paper [24], we have discussed how the probability of unknot should depend on the cylinder radius r for the self-avoiding polygons consisting of cylindrical segments with radius r . We note that the cylindrical self-avoiding polygons in Ref. [24] are constructed by the same method discussed in §2. Through numerical simulation, we have found that the unknotting probability denoted by $P_0(N, r)$ can be well described by the following:

$$P_0(N, r) = C_0(r) \exp(-N/N_0(r)), \quad (3.5)$$

where $C_0(r)$, $N_0(r)$ are fitting parameters. We note that this formula (3.5) corresponds to the special case of the general formula (3.4) when $K = 0$ and $m_K(r) = 0$. We note that the radius-dependence of the characteristic length $N_0(r)$ of unknot can be approximated by an exponential function of the cylinder radius r [24]:

$$N_0(r) \approx N_0(0) \exp(\alpha r). \quad (3.6)$$

We also note that the exponential dependence is favorable to the standard theory of polymers. [29]

3.3 Numerical estimates of knotting probability for the model of cylindrical self-avoiding polygons

Let us discuss the numerical data of the knotting probability obtained in our numerical simulations. For a given number N of nodes, we construct M cylindrical self-avoiding polygons with cylinder radius r by the dimerization method. Here M is given by $M = 10^4$, the polygonal nodes N from 50 to 1000 by 50 or 100, and the radius r from 0.0 to 0.007 by 0.001. (For details, see Figure Captions.) We have obtained numerical estimates of the knotting probabilities for the trivial knot, four prime knots ($3_1, 4_1, 5_1, 5_2$), and two composite knots ($3_1 \# 3_1, 3_1 \# 3_1 \# 3_1$). We note that we shall also discuss the knotting probabilities of small sized self-avoiding polygons such as $N = 20$ or 30 by the cylindrical ring-dimerization method. In §4, the connection to the hedge-hog method is studied.

In Fig. 4, the estimates of the knotting probability $P_0(N, r)$ for the trivial knot are plotted against the number N of nodes with $r=0.001, 0.003, 0.005$. The lines in Fig. 4 are theoretical curves given by the formula (3.5). We confirm the exponential decay of $P_0(N, r)$ also for the cylindrical self-avoiding polygons with large numbers of nodes which are constructed by the dimerization method. (See also Ref.[24].)

In Fig. 5, the numerical values of the knotting probabilities $P_K(N, r)$ are plotted against the step number N for the prime knots $3_1, 4_1, 5_1$. We see from Fig. 5 that the majority of nontrivial prime knots are given by the trefoil knots (3_1). We also observe that the peak values of the knotting probabilities decrease as the cylinder radius r increases. There is also a tendency for the prime knots that knots with larger crossing number have less peak values.

In Fig. 6, we show our estimates of the knotting probabilities of knots 5_1 and 5_2 versus the number N of nodes. We see that the knotting probability of the knot 5_2 is always larger than that of the knot 5_1 . However, for both the two knots the knotting probabilities have their maximal values at almost the same number N of nodes. Here we note that the error bars of Fig. 6 correspond to half of the values of the standard deviations of the knotting probability: In Figs. 4, 5 and 7, the error bars present the standard deviations of the knotting probability, while in Fig. 6 they show half of the values since they are too large to be depicted. We discuss how we have evaluated the “standard deviations” later in §3.3.

In Fig. 7, the knotting probabilities of two composite knots $3_1 \# 3_1$ and $3_1 \# 3_1 \# 3_1$, are plotted against the number N of nodes for the values of the cylinder radius r given by $r=0.001, 0.003, 0.005$. The knotting probabilities of the two composite knots have their maxima at different values of the number N of nodes, which are also different from that of the prime knots.

In Figs. 5-7 of the knotting probabilities, all the fitting curves are given by the formula (3.4). From the Figures, we see that it gives good fitting curves to the graphs of the knotting probability $P_K(N, r)$ versus the number N of nodes for the cylindrical self-avoiding polygons with the different values of the radius r . The least-square estimates of the parameters $m_K(r)$, $C_K(r)$, and $N_K(r)$ for the fitting curves are listed in Table 2 together with their χ^2 values. The errors for the best estimates of the parameters given in Table 2 correspond to 68.3 % confidence intervals, which are equivalent to the standard deviations.

Let us explain the method for evaluating the errors of the estimates of the knotting probabilities: with the error values, we have determined the fitting curves shown in Figs. 4-7. Throughout the paper,

we estimate the error of the knotting probability $P_K(N, r)$ by the following method: taking the sum of the contributions from the statistical fluctuation of the number M_K and that of statistical weight appearing in the ring-concatenating procedure (i.e., the ring-dimerization process in §2.3), multiplying the sum by the factor of 2, and then we regard the result as the error corresponding to the standard deviation of the knotting probability $P_K(N, r)$. It seems that this method of evaluating errors might give larger values of errors than other methods. However, we have employed it in order to compensate some possibly neglected contributions to the errors arising from the chain-dimerization process. It would be not easy to estimate the possible errors in the dimerization process, systematically. In fact, we do not take into account any possible statistical fluctuation in the dimerization process for constructing cylindrical self-avoiding chains. It could be as large as that of the statistical weight in the ring-concatenating procedure.

We make a comment on the dimerization process. Giving one initial number to the generator of pseudo-random numbers, we construct $M = 10^4$ cylindrical self-avoiding polygons with number N of nodes and radius r . This method makes our simulation simpler and more practical than giving several different initial numbers to the generator. However, it might give slightly larger values of errors. This consideration has been reflected in our method for estimating errors discussed in the last paragraph.

3.4 Some novel properties of fitting parameters

Let us discuss the best estimates of the fitting parameters $N_K(r)$, $m_K(r)$ and $C_K(r)$ listed in Table 2. From the list, we can derive a number of important observations for the fitting parameters.

First, we consider the values of the parameter $C_K(r)$. From Table 2, we see that the values of $C_K(r)$ are almost independent of the cylinder radius r , within the error bars. Thus we may have the conjecture that the parameter $C_K(r)$ should be a constant with respect to the radius r for any knot K :

$$C_K(r) \simeq C_K(0). \quad (3.7)$$

The parameter $C_K(0)$ of a knot K must reflect at least some kind of complexity of the knot. In fact, the probability of observing the knot type K is small when the value of $C_K(0)$ is small. Furthermore, as far as the prime knots are concerned, there seems to be a tendency that a knot with a smaller value of the knotting probability is likely to be more complex. Furthermore, the value of the parameter $C_K(0)$ is not directly related to the crossing number of the knot K . For instance, the value of $C_{5_1}(0)$ is smaller than that of $C_{5_2}(0)$ although both of the knots 5_1 and 5_2 have the same crossing number.

Second, we consider the characteristic length $N_K(r)$. Let us discuss how the parameter $N_K(r)$ should depend on the cylinder radius r for a given knot type K . From Fig. 8, we see that $N_K(r)$ can be approximated by an exponential function of the chain thickness r : $N_K(r) = N_K(0) \exp(\alpha_K r)$, at least for the trivial knot $K = 0$ and the trefoil knot $K = 3_1$. Considering the poor statistics for the case of the nontrivial knots, we may conjecture that $N_K(r)$ should depend on r exponentially for any knot K . Let us next discuss the knot-dependence of the parameter $N_K(r)$ with the radius r fixed. From Fig. 9, we see that the values of the parameters $N_K(r)$ for the different knots are almost given by the same value with respect to the errors.

Combining the results of the radius- and knot-dependence of the parameter $N_K(r)$, we have the conjecture that the parameter $N_K(r)$ for a knot K should be equal to that of the trivial knot and also that it should be given by an exponential function of the cylinder radius r : $N_K(r) = N_0(0) \exp(\alpha_0 r)$.

In fact, in the previous paper [24], we calculated the probability of observing the trivial knot from the values of the cylinder radius r from 0.0 to 0.1 by 0.01, and discussed how the parameter $N_0(r)$ should depend on the cylinder radius r . Then, we found that the characteristic length $N_0(r)$ is roughly approximated by an increasing exponential function of r as $N_0(r) = N_0(0) \exp(\alpha r)$, with $N_0(0) = 292 \pm 5$, and $\alpha = 43.5 \pm 0.6$. We note that $\chi^2=42$ while the number of data points is ten with the two fitting parameters. In order to improve the χ^2 value, we have also considered another fitting formula $N_0(r) = N_0(0) \exp(\beta r^\nu)$, where there are three parameters to fit $N_0(0)$, β , and ν . The best estimates of the fitting parameters are given by $N_0(0)=271 \pm 6$, $\beta = 29 \pm 2$, $\nu = 0.85 \pm 0.02$, and the χ^2 value is given by 2.2.

The results of the previous paper [24] are consistent with that of the trivial knot in this paper. We note that the range of the cylinder radius r in the present paper is much narrower than that of Ref. [24]. Here, we consider the values of the cylinder radius from 0.001 to 0.007 by 0.001. Even the second fitting function: $N_0(r) = N_0(0) \exp(\beta r^\nu)$ can also be approximated by an exponential function of r . However, the connection between the formulas (3.4) and (1.2)(or (4.1)) can be shown more clearly by the first fitting formula than by the second one as we shall show in §4. Thus, we employ the first one in the paper.

Third, we discuss the exponent $m_K(r)$ of a knot K . From Table 2, we see that the values of the parameter $m_K(r)$ should be independent of the cylinder radius r for any knot K . This property is consistent with the conjecture that the exponent m_K of a knot K should be universal, which was also investigated for the rod-bead model of self-avoiding polygons and the Gaussian model of random poly-

gons. [16] Furthermore, within the error bars, the values of the exponents can be roughly approximated as follows: $m_K(r) \simeq 0$ for the trivial knot ($K = 0$); $m_K(r) \simeq 1$ for the four prime knots 3_1 , 4_1 , 5_1 and 5_2 ; $m_K(r) \simeq 2$ for the composite knot $3_1 \# 3_1$; $m_K(r) \simeq 3$ for the composite knot $3_1 \# 3_1 \# 3_1$. It is interesting to note that the roughly approximated values of $m_K(r)$ are consistent with the results not only of the off-lattice models such as the Gaussian model [14] and the rod-bead model [15], but also of the lattice model [17] of self-avoiding polygons. The roughly approximated values are also consistent with the additivity of the exponent m_K that the exponent of a composite knot should be given by the sum of the exponents of the constituent prime knots: $m(K_1 \# K_2) = m(K_1) + m(K_2)$ and so on, which was first observed for the Gaussian model of random polygons. [14]

Let us discuss an interesting consequence of the conjectures on the fitting parameters given in the above. We first note that among the three fitting parameters, only the characteristic length $N_K(r)$ should depend on the cylinder radius r ; the other two parameters should be independent of it. We recall also the conjecture that $N_K(r) = N_0(r)$ for any knot K . Thus, if we assume that the value of the exponent m_K can be approximated by the same value for any prime knot K , then we have the following relation between the knotting probabilities of any two prime knots K_1 and K_2 :

$$P_{K_1}(N, r)/P_{K_2}(N, r) \simeq C_{K_1}/C_{K_2}. \quad (3.8)$$

Thus, the ratio of the knotting probabilities of any two prime knots K_1 and K_2 should be roughly given by that of the parameters C_{K_1} and C_{K_2} .

4 Topological Entropy and Random Knotting of Circular DNAs

4.1 Probability of random knotting of circular DNAs

In this section, we discuss the connection of the knotting probability to some experiments of DNA random knots [19, 20].

Let us consider DNA molecules in an electrolyte solution. The DNAs are polyelectrolytes with negative charges, and the DNA chains are surrounded by some clouds of counter ions. Partially due to the electrostatic repulsion among the chains, they are considered as stiff chains; in fact, the Kuhn statistical length of DNA chains is given by rather a large value, about 50 nm [18].

In order to study thermodynamic properties of DNA chains we can simulate the DNA chains by some configurations of wormlike chains with the

effective diameter corresponding to the screening length [21, 23]. For any wormlike chain, the persistent length (i.e., the Kuhn length) is fundamental. The length of a wormlike chain should be expressed in terms of the Kuhn statistical unit. Thus, we can replace wormlike chains by such self-avoiding walks that have cylindrical segments with the persistent length. Let us now consider wormlike rings which are given by rings made of wormlike chains. Then, we can also approximate wormlike rings by such self-avoiding polygons consisting of cylindrical segments with some effective diameter whose length is given by the Kuhn length [11].

Let us discuss the algorithm for generating cylindrical self-avoiding polygons which we call the hedge-hog method of ring polymers. [11] The algorithm is given by the following: we generate a set of vectors of unit length with a common origin (a “hedge-hog”), and applying the Monte-Carlo procedure to the set, we derive a random sequence of self-avoiding polygons, keeping only those configurations that have no overlap between any two unadjacent cylindrical segments. (See §A.2)

Through the numerical simulations, the probability of being knotted has been evaluated for the hedge-hog method [11]. For the data, the radius-dependence of the probability $P_{knotted}(N, r)$ has been well approximated by the empirical formula (1.2). Furthermore, a different method of wormlike polygons has been introduced, which we call the MC method with the bending energy (See §A.3) [19], and the knotting probabilities of two prime knots 3_1 and 4_1 are evaluated for the wormlike rings with N Kuhn lengths, where N is given from 16 to 60. For a given nontrivial knot K , let the symbol $P_K(N, r)$ denote the knotting probability of the wormlike rings, which are constructed by the MC method with the bending energy with the chain radius r consisting of N units of the Kuhn length b . Then, the data are fitted by the following formula:

$$P_K(N, r) = P_K(N, 0) \exp(-\gamma_K \frac{r}{b}) \quad (4.1)$$

Here, γ_K is a constant which is independent of N and to be determined by the simulation for each nontrivial knot K [19].

The knotting probability of the wormlike rings of the MC method with the bending energy is consistent with that of the hedge-hog method; the knotting probability of wormlike rings of the MC method with the bending energy consisting of N Kuhn units with the cylinder radius r should be equivalent to the hedge-hog method with N cylindrical segments with radius r . In fact, it was discussed in Ref. [19] that the knotting probability of a particular knot for the wormlike ring can be determined by the number N of Kuhn statistical units and the chain radius r . In general, for any model of wormlike rings, the Kuhn statistical length b is not

necessarily equivalent to the length of one segment of the rings; it can be much longer than the length of the segments, such as the case of the MC method with the bending energy.

The empirical formulae (1.2) and (4.1) give the connection of the knotting probability to experiments of DNA random knots. V.V. Rybencov *et.al.* and S. Y. Shaw and J.C. Wang measured the fractions of knotted species generated by the method of random ring closure of DNAs through the electrophoretic separation method. [19, 20] The effective diameter of the DNA double helix was evaluated, by comparing the knotted fractions observed in the experiments with the theoretical estimates of the knotting probability given by the computer simulations [11] of the hedge-hog method. [19, 20]

4.2 Consistency of knotting probabilities for dimerization and hedge-hog methods

We now discuss that the hedge-hog and dimerization methods for constructing cylindrical self-avoiding polygons are consistent as far as their knotting probabilities are concerned. Let us consider our numerical estimates of the probability $P_{knotted}(N, r)$ of being knotted for the hedge-hog and dimerization methods, which are obtained in our simulations. Here, we set $b = 1$ for the hedge-hog method without any loss of generality.

For the hedge-hog method, we have evaluated the probability $P_{knotted}(N, r)$ for the cases of $N=20$ and 30 . For the dimerization method, we have evaluated it for the cases of $N=21$ and 31 . For each of the methods, the values of the diameter $2r$ are given by the values from 0.0 to 0.05 by 0.01 .

Our numerical estimates of the probability $P_{knotted}(N, r)$ of the hedge-hog method gives almost the same with that of Ref. [11]. Furthermore, our estimates of the probability $P_{knotted}(N, r)$ of the hedge-hog method is also consistent with that of the dimerization method. We have thus confirmed that the data of the probability $P_{knotted}(N, r)$ of the cylindrical self-avoiding polygons of the dimerization method satisfy the empirical formula (1.2) for the thickness-dependence of the knotting probability, for the small numbers N of nodes.

4.3 Limited validity of the empirical formula for the knotting probability of DNAs

We recall that the empirical formula (4.1) describing the thickness-dependence of the knotting probability has been fundamental in the study of the random knots of circular DNAs. However, we shall show that it is not valid when the number N of nodes is large enough.

Let us consider the N -dependence of the ratio: $P_K(N, r)/P_K(N, 0)$ of the knotting probability for a given nontrivial knot K . If the empirical formula (4.1) should be valid, then the ratio would be given by the following:

$$P_K(N, r)/P_K(N, 0) = \exp(-\gamma_K r/b). \quad (4.2)$$

We note that it should be constant with respect to N .

In Fig. 11, the data of $P_K(N, r)/P_K(N, 0)$ for the region of r from $r=0.001$ to $r=0.007$ by 0.001 are plotted against the number N of nodes. Then, we see that the ratio is not constant but increases with respect to N . Thus, the formula (4.1) does not hold when the number N of nodes is large enough such as $N > 100$.

We make a comment on the method for estimating the errors shown in Fig. 11. We note that the error bars denote the standard deviations in Fig. 11. The variance σ^2 of the ratio: $P(N, r)/P(N, 0)$ is given by the following formula:

$$\sigma^2 = \frac{1}{P(N, 0)^2} \left\{ \sigma_1^2 + \left(\frac{P(N, r)}{P(N, 0)} \right)^2 \sigma_2^2 \right\} \quad (4.3)$$

Here σ_1 denotes the variance of $P(N, r)$ and σ_2 that of $P(N, 0)$.

4.4 Reduction of the scaling formula of knotting probability in the case of small N

Let us explicitly discuss how the generalized scaling formula (3.4) is related to the empirical formula (4.1). In fact, this gives a kind of “extrapolation” of the scaling formula into a region of small N . The scaling formula should be valid when N is very large, since it is nothing but an asymptotic expansion with respect to N . On the other hand, the empirical formulae (1.2) and (4.1) should be valid only for some small number N of nodes.

There are three points in our discussion. First, we recall that the parameter $C_K(r)$ should be independent of the cylinder radius r : $C_K(r) \simeq C_K(0)$. Then, from the formula (3.4), we have the following expression for the ratio of $P_K(N, r)$ to $P_K(N, 0)$:

$$\frac{P_K(N, r)}{P_K(N, 0)} = \left(\frac{N_K(0)}{N_K(r)} \right)^{m(K)} \exp \left(\frac{N}{N_0(0)} - \frac{N}{N_0(r)} \right) \quad (4.4)$$

Second, we can neglect the exponential factor in the right-hand-side of (4.4), when N is small such as $N \leq 30$. The characteristic length $N_K(r)$ can be roughly evaluated as $N_K(r) \geq 300$ when r is given by some value from 0.001 to 0.01 . The value is about ten times larger than that of the number N of nodes, when $N < 30$. Therefore, the exponential argument $\frac{N}{N_0(0)} - \frac{N}{N_0(r)}$ should be rather small. Third,

we recall that the characteristic length $N_0(r)$ can be given by $N_0(r) \simeq N_0(0) \exp(\alpha r)$, as discussed in §3.4 (see also in the previous paper: [24]). Furthermore, we may assume the conjecture that the characteristic lengths do not depend on any knot type K : $N_K(r) \simeq N_0(r)$. Combining the three points given in the above, we see that the main contribution to the ratio of eq. (4.4) is given by

$$\frac{P_K(N, r)}{P_K(N, 0)} \simeq \exp(-\alpha m_K r) \quad (4.5)$$

We note that the factor $(N_K(0)/N_K(r))^{m_K}$ should correspond to the exponential factor $\exp(-\gamma_K r/b)$ in the empirical formulae (1.2) and (4.1). Explicitly, we have $\gamma_K = \alpha m_K$ when $b = 1$. Thus it is shown that the empirical formula (1.2) can be derived from the generalized scaling formula (3.4). We recall that the constant γ_K is assumed to be independent of N in Ref. [19].

We remark that the knotting probability $P_K(N, r)$ can be described by the generalized scaling formula (3.4) from small N to large N , as shown in §3.3, explicitly. Furthermore, if we assume the properties $C_K(r) \simeq C_K(0)$, $N_K(r) \simeq N_0(r)$ and $N_0(r) \simeq N_0(0) \exp(\alpha r)$, then we have the following expression

$$\log \left(\frac{P_K(N, r)}{P_K(N, 0)} \right) \simeq -\alpha m_K r + \frac{N}{N_0(0)} (1 - \exp(-\alpha r)), \quad (4.6)$$

which is consistent with the N -dependence shown in Fig. 11, within error bars.

For the case of the trivial knot, we may also consider the r -dependence of the second factor of the right-hand-side of eq. (4.4), which can be neglected for the case of nontrivial knots. Taking into account the fact that $m_0 \simeq 0$, we have the following approximation:

$$\frac{P_0(N, r)}{P_0(N, 0)} \simeq \exp \left(\frac{N}{N_0(0)} (1 - \exp(-\alpha r)) \right). \quad (4.7)$$

Here we note that the r -dependence of the unknotting probability has not been discussed previously, yet.

5 Concluding Remarks

In this paper we have discussed how the knotting probability (or equivalently, the topological entropy) should depend on the cylinder radius for the cylindrical self-avoiding polygons. The dimerization and hedge-hog methods give almost the same values for the knotting probability, although their algorithms are quite different. This coincidence suggests that any algorithm of cylindrical self-avoiding polygons with N Kuhn statistical units and the cylinder radius r may give essentially the same value for the knotting probability. We have also found

that for any knot investigated, the knotting probability of the model of cylindrical self-avoiding polygons is described by the generalized scaling formula (3.4) as a function of the number N of nodes and the cylinder radius r .

From the best estimates of the fitting parameters, we have observed several important properties of the parameters. Based on these properties, we can derive a conjecture of the best formula of the knotting probability. For self-avoiding polygons with N cylindrical segments with the radius r of unit length, the best formula of the knotting probability for knot K is given by the following:

$$P_K(N, r) = C_K (N/N_c(r))^{m_K} \exp(-N/N_c(r)), \quad (5.1)$$

where the characteristic length $N_c(r)$ is independent of knots and is given by

$$N_c(r) = N_c(0) \exp(\alpha r). \quad (5.2)$$

We recall that C_K and m_K should be constant with respect to the cylinder radius r . We shall investigate the conjecture more precisely in later publications.

Finally, we make a comment on the range of r . In the paper, we have discussed for some nontrivial knots the knotting probabilities of the cylindrical self-avoiding polygons with radius r given from 0 to 0.007. On the other hand, in Ref. [24], we have discussed the probability of unknot for the wider range of r : from 0 to 0.1. From the result of Ref. [24], it is suggested that the conjecture (5.1) should be valid also for the larger values of radius r . Thus, it is an interesting future problem to check the conjecture explicitly through numerical simulations.

References

- [1] F.B. Dean, A. Stasiak, T. Koller and N.R. Cozzarelli: J. Biol. Chem. **260** (1985) 4795; S.A. Wasserman, J.M. Duncan and N.R. Cozzarelli: Science **229** (1985)171; Science **232** (1986) 951.
- [2] K. Shishido, N. Komiyama and S. Ikawa: J. Mol. Biol. **195** (1987) 215.
- [3] D.M. Walba, Tetrahedron: **41** (1985) 3161.
- [4] M. Delbück: *Mathematical Problems in the Biological Sciences*, edited by R.E. Bellman: Proc. Symp. Appl. Math **14** (1962) 55.
- [5] H.L. Frisch and E. Wasserman: J. Amer. Chem. Soc. **83** (1961) 3789.
- [6] A.V. Vologodskii, A.V. Lukashin, M.D. Frank-Kamenetskii, and V.V. Anshelevich: Sov. Phys. JETP **39** (1974) 1059.

- [7] J. des Cloizeaux and M.L. Mehta: J. Phys. (Paris) **40** (1979) 665.
- [8] J.P.J. Michels and F.W. Wiegel: Phys. Lett. A **90** (1982) 381.
- [9] M. Le Bret: Biopolymers **19** (1980) 619.
- [10] Y.D. Chen: J. Chem. Phys. **74** (1981) 2034; J. Chem. Phys. **75**, 2447 (1981); J. Chem. Phys. **75** (1981) 5160.
- [11] K.V. Klenin, A.V. Vologodskii, V.V. Anshelevich, A.M. Dykhne and M.D. Frank-Kamenetskii: J. Biomol. Struct. Dyn. **5**(1988) 1173.
- [12] E.J. Janse van Rensburg and S.G. Whittington: J.Phys. A **23** (1990) 3573.
- [13] K. Koniaris and M. Muthukumar: Phys. Rev. Lett. **66** (1991) 2211.
- [14] T. Deguchi and K. Tsurusaki: J. Knot Theory and Its Ramifications **3** (1994) 321.
- [15] T. Deguchi and K. Tsurusaki: *Geometry and Physics*, Lect. Notes in Pure and Applied Math. Series/184, ed. by J.E. Andersen, J. Dupont, H. Pedersen, and A. Swann, (Marcel Dekker Inc., Basel Switzerland, 1997), pp. 557-565. (the Proceedings of *Geometry and Physics*, Institute of Mathematics, University of Aarhus, 18th-27th July, 1995, Aarhus, Denmark.)
- [16] T. Deguchi and K. Tsurusaki: Phys. Rev. E **55** (1997) 6245.
- [17] E. Orlandini, M.C. Tesi, E.J. Janse van Rensburg and S.G. Whittington: J. Phys. A: Math. Gen. **31** (1998) 5953.
- [18] A.Yu. Grosberg and A.R. Khokhlov: *Statistical Physics of Macromolecules*, AIP Press, 1994.
- [19] V.V. Rybenkov, N.R. Cozzarelli and A.V. Vologodskii: Proc. Natl. Acad. Sci. USA **90** (1993) 5307.
- [20] S.Y. Shaw and J.C. Wang: Science **260** (1993) 533.
- [21] D. Stiger: Biopolymer **16** (1977) 1435.
- [22] A.A. Brian, H.L. Frisch and L.S. Lerman: Biopolymer **20**, (1981) 1305.
- [23] T. Odijk: J. Poly. Sci.: Polym. Phys. **15** (1977) 477; J. Skolnick and M. Fixman: Macromolecules **10** (1977) 944.
- [24] M.K. Shimamura and T. Deguchi: preprint cond-mat/0008268, Phys. Lett. A **274** (2000) 184.
- [25] T. Deguchi and K. Tsurusaki: Phys. Lett. A **174** (1993) 29;
See also, M. Wadati, T. Deguchi and Y. Akutsu: Phys. Reports **180** (1989) 247; V.G. Turaev: Math. USSR Izvestiya **35** (1990) 411.
- [26] M. Polyak and O. Viro: Int. Math. Res. Not. No.11 (1994) 445.
- [27] N. Madras and G. Slade: *The Self-Avoiding Walk*, (Birkhäuser, Boston, 1993), §9.3.2.
- [28] P.G. de Gennes: *Scaling Concepts of Polymer Physics* (Cornel University Press, Ithaca, 1979).
- [29] A. Grosberg and S. Nechaev: J. Phys. A: Math. Gen. **25** (1992) 4659.

Appendix A: Algorithms for the Model of Ring Polymers

In Appendix A, we describe the three different algorithms for constructing self-avoiding polygons consisting of freely jointed hard cylinders.[24, 11, 19] All the three algorithms should produce equivalent sets of ring polymers corresponding to the discrete worm-like chains, if the numbers of polygons constructed are very large. As far as constructing large polygons, however, it seems that the dimerization algorithm should be the most efficient.

A.1 Cylindrical ring-dimerization method (the dimerization method)

Let us explicitly discuss the method for generating ring polymers of freely jointed hard cylinders, by which almost all the polygons in the paper are constructed. The method is based on the algorithm of Ref. [10] for the rod-bead model. It consists of three parts: (1) generation of basic chains of hard cylinders; (2) propagation of linear chains by the dimerization algorithm; (3) formation of ring polymers by connecting two linear chains. We call the combined procedure of the parts (1), (2) and (3), the cylindrical ring-dimerization method.

Basic chains consisting of hard cylinders are generated by the straightforward Monte Carlo method. For an illustration, let us suppose that we make basic chains of eight cylindrical segments. Then, for any pair of unadjacent cylinders, we check the overlapping condition between the cylinders which is described in Appendix B. If there is a pair satisfying the overlapping condition in a given basic chain, then we throw away the whole chain and start from the beginning. If we find that there is no overlapping pair of unadjacent cylinders, then we store the chain in a computer disk. Here we recall that we do not check the overlapping condition for any pair of adjacent cylinders. This corresponds to the freely-jointedness of the model.

Let us consider how to make chains of sixteen cylinders. We make two pools of M basic chains in the disk. Then, we choose randomly basic chains 1 and 2 from the first and second pools, respectively. We join them together by placing the zeroth node of the second chain on the eighth node of the first chain. If there is no overlapping pair of unadjacent cylinders in the new chain of sixteen cylinders, then we store it in the computer disk. If there is any overlapping unadjacent pair, then we throw it away. We thus construct M chains of sixteen cylinders in the disk. The same procedure is used for creating chains of, say, 32 cylinders, 64 cylinders, etc. We note that chains with any number of cylinders can be constructed by the dimerization scheme shown in Fig. 3.

Let us describe the procedure of making ring polymers of $2N + 1$ cylinders from linear chains of N cylinders. We consider two pools S_1 and S_2 of M chains of freely jointed N hard cylinders. We pick up randomly chain 1 in the pool S_1 . Then, we can choose chain 2 randomly in the pool S_2 . In order to make the process more efficient, however, we choose chain 2 as follows. Let the symbols h_1 and h_2 denote the end-to-end distances of chains 1 and 2, respectively. Here we recall that the length of cylindrical segments is given by 1. Then, we choose chain 2 randomly from the group of chains in S_2 which satisfy the condition:

$$|h_1 - 1| \leq h_2 \leq h_1 + 1. \quad (\text{A.1})$$

The sampling bias induced by this operation is corrected with the statistical weight m/M , where m is the number of chains in S_2 which satisfy the condition (A.1). We recall that M is the total number of linear chains in S_2 .

Let us put a new cylindrical segment between the two ends of the chains 1 and 2. Then, we check whether there exists any segment in the two chains which overlaps with the new segment, except for the two neighboring ones. We also check the overlapping condition for every unadjacent pair of cylinder in which are cylinder is in chain 1 and another in chain 2. If there is no overlap, then we consider that the selected pair of chains makes a perfect ring with $2N + 1$ cylindrical segments. We store the ring in the hard disk. However, the probability of forming a ring depends on the values of h_1 and h_2 . Let us denote by θ the angle between the end-to-end vectors of the two chains 1 and 2. Then, the probability is proportional to $2\pi \sin \theta$. We note that $2\pi h_2 \sin \theta$ is the arclength of the circle on which the end-point of the chain 2 can be placed. The probability of forming a ring should be proportional to the arclength of the circle divided by h_2 . Thus, the total statistical weight of the ring-dimerization procedure is given by

$$W = \frac{m}{M} \sin \theta \quad (\text{A.2})$$

Here, the angle θ is determined by the values h_1 and h_2 as follows

$$\cos \theta = \frac{h_1^2 + h_2^2 - 1}{2h_1 h_2} \quad (\text{A.3})$$

We remark that all the expectation values of some quantities of the model such as the knotting probability etc., should be calculated by taking the weighted averages with respect to the statistical weight of eq. (A.2).

A.2 Monte-Carlo method with random hedgehog (the hedge-hog method)

Let us describe the algorithm of Ref. [11], which we call the Monte-Carlo method with random hedgehog, or the hedgehog method, for short. First, a set of n (even number) vectors e_i of unit length with a common origin (a ‘‘hedgehog’’) is generated as follows: In the hedgehog, for those vectors that have odd i values, their directions are chosen randomly and independently; for even i values, we set $e_i = -e_{i-1}$. Thus, we have $\sum_{i=1}^n e_i = 0$. Then, to exclude pair correlations between the vectors, for each e_i , we choose a different vector e_j randomly from the hedgehog and the pair of vectors e_i and e_j are rotated at a random angle around the bisectrix of the angle between them. This operation does not change the sum $e_i + e_j$, and the sum of all the vectors in the hedgehog remains zero, consequently. The process is repeated for each vector of the random hedgehog, many times. As a result, a ‘‘random hedgehog’’ is obtained. Then, the vectors of the random hedgehog are put in an arbitrary order, and we have the chain. The resulting chain is automatically closed.

In order to take into account the excluded volume effect, chain segments are modeled as hard cylinders with radius r . We generate a large number of closed chains by the random hedgehog method, and then retained only those of them for which the minimum distance between any two unadjacent segments is larger than the segment diameter $2r$.

A.3 Monte-Carlo method with the bending energy

We consider the algorithm of Ref. [19], which we call the Monte-Carlo method with the bending energy. A closed chain of kn segments of rigid impenetrable cylinders of equal length and radius r is constructed. Here k elementary segments correspond to the Kuhn statistical length, and the closed chain consists of n Kuhn segments. The conformational sets are obtained by successive deformations of a starting conformation in accordance with the Metropolis-Monte Carlo procedure. The deformation is rotation of a subchain containing an arbitrary

trary number of adjacent segments by a randomly chosen angle, ϕ , around the straight line connecting the vertices bounding the subchain. The value of ϕ is uniformly distributed over an interval $(-\phi_0 \text{ to } \phi_0)$, where the interval is chosen so that about half of the moves are accepted. It depends on the energy whether a trial conformation generated is accepted or not. The energy of the chain, E , is calculated as

$$E = RT\alpha \sum_{i=1}^{kn} \theta_i^2 \quad (\text{A.4})$$

where summation is done over all the joints between the elementary segments, R is the gas constant, T is the absolute temperature, θ_i is the angular displacement of the i th segment relative to segment $i-1$, and α is the bending rigidity constant. The bending rigidity constant is chosen so that exactly k elementary segments correspond to the Kuhn statistical segment length. For each set of values of n and r , a large number of conformations are generated.

Appendix B: Overlapping Condition of the Cylinder Model

We discuss the condition when a given pair of cylinder segments with radius r has an “overlap”, explicitly. We first recall that the central line segment of a cylinder is defined by the line segment between the centers of the upper and lower disks of the cylinder. We now define the condition of an “overlap” as follows: given two cylinder segments are said to have an “overlap” if and only if the distance between their central line segments is less than the cylinder diameter $2r$.

Let us formulate the algorithm for the overlapping condition. We consider a pair of two cylinders with radius r and unit length in three dimensions. We may assume that the end points of their central line segments are given by \vec{b} and $\vec{a} + \vec{b}$, \vec{d} and $\vec{c} + \vec{d}$, respectively. Here, the vectors \vec{a} and \vec{c} are unit vectors. Then, any point on the central line segments can be expressed by \vec{X}_s or \vec{X}_t given in the following:

$$\vec{X}_s = s\vec{a} + \vec{b} \quad \vec{X}_t = t\vec{c} + \vec{d} \quad (\text{B.1})$$

where s and t are real parameters satisfying $0 \leq s, t \leq 1$. We also define the angle parameter θ by the relation: $\vec{a} \cdot \vec{c} = \cos \theta$, where we take the branch: $0 \leq \theta \leq \pi$.

Let us consider the two infinite lines extending the two central line segments for \vec{X}_s and \vec{X}_t , respectively. Then, the distance between the two infinite lines is given by the minimum of the quantity: $D = |\vec{X}_s - \vec{X}_t|$. Denoting the minimum distance by D_{min} , we have

$$D_{min}^2 = -s_m^2 - t_m^2 + 2s_mt_m \cos \theta + \gamma, \quad (\text{B.2})$$

where the parameters s_m and t_m are given by

$$s_m = \frac{1}{\sin^2 \theta} (\alpha + \beta \cos \theta), \quad t_m = \frac{1}{\sin^2 \theta} (\alpha \cos \theta + \beta). \quad (\text{B.3})$$

Here α , β , and γ have been defined by $\alpha = -\vec{a} \cdot (\vec{b} - \vec{d})$, $\beta = \vec{c} \cdot (\vec{b} - \vec{d})$, and $\gamma = (\vec{b} - \vec{d})^2$, respectively. We note that s_m and t_m are such values of the parameters s and t that give the minimum D_{min} for $D = |\vec{X}_s - \vec{X}_t|$.

Let us now explain the algorithm. First we calculate the value of $\cos \theta$. Here, we suppose that $\cos^2 \theta < 1$, and we shall consider the case when $\cos^2 \theta = 1$, later. If D_{min} is larger than the diameter $2r$, then there is no overlap between the two cylinder segments. If D_{min} is smaller than $2r$, we check the values of s_m and t_m . If $0 \leq s_m \leq 1$ and $0 \leq t_m \leq 1$, there is an overlap; otherwise, we choose the value d_{min}^2 , which will be given shortly, and we calculate $D_{sum}^2 = d_{min}^2 + D_{min}^2$. If D_{sum} is larger than $2r$, then there is no overlap; otherwise, there is an overlap.

Let us now formulate the value d_{min}^2 , explicitly. We first define z_j for $j = 0, 1, 2, 3$, in the following:

$$\begin{aligned} z_0 &= s_m - t_m \cos \theta \\ z_1 &= t_m - s_m \cos \theta \\ z_2 &= z_0 + \cos \theta \\ z_3 &= z_1 + \cos \theta \end{aligned} \quad (\text{B.4})$$

Then, we define p_j for $j = 0, 1, 2, 3$ as follows:

$$\begin{aligned} p_0 &= \begin{cases} z_0^2 + t_m^2 \sin^2 \theta & \text{for } z_0 < 0 \\ t_m^2 \sin^2 \theta & \text{for } 0 \leq z_0 \leq 1 \\ (1 - z_0)^2 + t_m^2 \sin^2 \theta & \text{for } z_0 > 1 \end{cases} \\ p_1 &= \begin{cases} z_1^2 + s_m^2 \sin^2 \theta & \text{for } z_1 < 0 \\ s_m^2 \sin^2 \theta & \text{for } 0 \leq z_1 \leq 1 \\ (1 - z_1)^2 + s_m^2 \sin^2 \theta & \text{for } z_1 > 1 \end{cases} \\ p_2 &= \begin{cases} z_2^2 + (1 - t_m)^2 \sin^2 \theta & \text{for } z_2 < 0 \\ (1 - t_m)^2 \sin^2 \theta & \text{for } 0 \leq z_2 \leq 1 \\ (1 - z_2)^2 + (1 - t_m)^2 \sin^2 \theta & \text{for } z_2 > 1 \end{cases} \\ p_3 &= \begin{cases} z_3^2 + (1 - s_m)^2 \sin^2 \theta & \text{for } z_3 < 0 \\ (1 - s_m)^2 \sin^2 \theta & \text{for } 0 \leq z_3 \leq 1 \\ (1 - z_3)^2 + (1 - s_m)^2 \sin^2 \theta & \text{for } z_3 > 1 \end{cases} \end{aligned} \quad (\text{B.5})$$

Then, we define d_{min}^2 by the minimum of p_j for $j = 0, 1, 2, 3$.

Finally, we discuss the case when $\theta = 0$ or π . When $\theta = 0$, we define D_{min}^2 by

$$D_{min}^2 = \begin{cases} 1 + 2\alpha + \gamma & \text{for } \alpha < -1 \\ \gamma - \alpha^2 & \text{for } -1 \leq \alpha \leq 2 \\ 1 - 2\alpha + \gamma & \text{for } \alpha > 2 \end{cases} \quad (\text{B.6})$$

When $\theta = \pi$, we define it by

$$D_{min}^2 = \begin{cases} \gamma & \text{for } \alpha < 0 \\ \gamma - \alpha^2 & \text{for } 0 \leq \alpha \leq 2 \\ 4 - 4\alpha + \gamma & \text{for } \alpha > 2 \end{cases} \quad (\text{B.7})$$

If D_{min} is greater than $2r$, we have no overlap; otherwise there is an overlap.

Figure Captions

Fig. 1: Trivial knot, prime knot 3_1 (trefoil knot), and composite knot $3_1 \# 3_1$. Knot $3_1 \# 3_1$ is given by a product of two prime knots 3_1 .

Fig. 2: Polygonal knot equivalent to trefoil knot 3_1 .

Fig. 3: Dimerization scheme for constructing self-avoiding walks of length 100; chains of lengths 12 and 13 are generated by a direct methods; then, chains of 25, 50 and 100 are given by the dimerization method, systematically.

Fig. 4: Unknotting probability $P_0(N, r)$ versus number N of polygonal nodes of the cylindrical self-avoiding polygons constructed by the dimerization method. Numerical estimates of $P_0(N, r)$ are shown for the following three values of r by black circles, black triangles and black diamonds, respectively: (a) $r=0.001, 0.003$ and 0.005 ; (b) $r=0.002, 0.004$, and 0.006 . Error bars denote their standard deviations. Number N of nodes are given by $51, 151$ and $100j + 1$ for $j = 1, 2, \dots, 10$.

Fig. 5: Knotting probability $P_K(N, r)$ of the cylindrical self-avoiding polygons constructed by the dimerization method versus number N of polygonal nodes for nontrivial prime knots. Numerical estimates of $P_K(N, r)$ for $K=3_1, 4_1$ and 5_1 are shown by black circles, black triangles and black diamonds, respectively, for the following values of r : (a) $r=0.001$; (b) $r=0.003$; (c) $r=0.005$. Error bars denote their standard deviations. Number N of nodes are given by $51, 151$ and $100j + 1$ for $j = 1, \dots, 10$.

Fig. 6: Knotting probability $P_K(N, r)$ of the cylindrical self-avoiding polygons constructed by the dimerization method versus number N of polygonal nodes for two knots with five crossings. Numerical estimates of $P_K(N, r)$ for $K=5_1$ and 5_2 are shown by black circles and black triangles, respectively, for the following values of r : (a) $r=0.001$; (b) $r=0.003$; (c) $r=0.005$. Error bars depicted in Fig. 6 are given simply by the sum of the statistical fluctuation of the number M_K and that of the statistical weight of the ring-dimerization procedure. Number N of nodes are given by $51, 151$, and $100j + 1$ for $j = 1, 2, \dots, 10$.

Fig. 7: Knotting probability $P_K(N, r)$ of the cylin-

drical self-avoiding polygons constructed by the dimerization method versus number N of polygonal nodes for two composite knots. Numerical estimates of $P_K(N, r)$ for $K = 3_1 \# 3_1$ and $3_1 \# 3_1 \# 3_1$ are shown by black circles and black triangles, respectively, for the following values of r : (a) $r=0.001$; (b) $r=0.003$; (c) $r=0.005$. Error bars denote their standard deviations. Number N of nodes are given by $51, 151$ and $100j + 1$ for $j = 1, 2, \dots, 10$.

Fig. 8: Semi-logarithmic plot of characteristic length $N_K(r)$ versus cylinder radius r of the cylindrical self-avoiding polygons constructed by the dimerization method. Numerical estimates of $N_K(r)$ for $K=0$ and 3_1 listed in Table 2 are depicted by black circles and black triangles, respectively, together with their error bars, with the values of r from 0.0 to 0.007 by 0.001 . All the black triangles (knot 3_1) are slightly shifted rightward by 0.0001 for graphical convenience. The straight fitting line is determined by the least square method.

Fig. 9: Semi-logarithmic plot of characteristic length $N_K(r)$ versus cylinder radius r of the cylindrical self-avoiding polygons constructed by the dimerization method. Numerical estimates of $N_K(r)$ for $K=0, 3_1, 4_1$, and 5_1 listed in Table 2 are depicted by black circles and black triangles, black diamonds and black crosses, respectively, for the values of r from 0.001 to 0.007 by 0.001 , together with their error bars. Black triangles (3_1), black diamonds (4_1) and black crosses (5_1) are shifted rightward by $0.0001, 0.0002$ and 0.0003 , respectively.

Fig.10: Probability $P_{knotted}(N, r)$ of being knotted versus cylindrical diameter $2r$ for the hedgehog and dimerization methods. Numerical estimates of $P_{knotted}(N, r)$ of the hedgehog method for $N = 20$ and 30 are shown by black circles and black triangles, respectively. Numerical estimates of $P_{knotted}(N, r)$ of the dimerization method for $N = 21$ and 31 are shown by black diamonds and black crosses, respectively. Error bars denote their standard deviations.

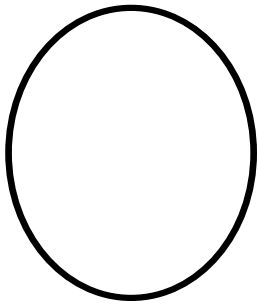
Fig. 11: The ratio $P_K(N, r)/P_K(N, 0)$ versus number N of polygonal nodes of the cylindrical self-avoiding polygons constructed by the dimerization method. Numerical estimates of $P_K(N, r)/P_K(N, 0)$ for $r = 0.001, 0.005$ and 0.007 are shown by black circles, black triangles and black diamonds, respectively, for the following knots: (a) trivial knot; (b) trefoil knot 3_1 .

Table 1: Values of the determinant of knot $|\Delta_K(-1)|$ and the second Vassiliev invariant $v_2(K)$ for some simple knots.

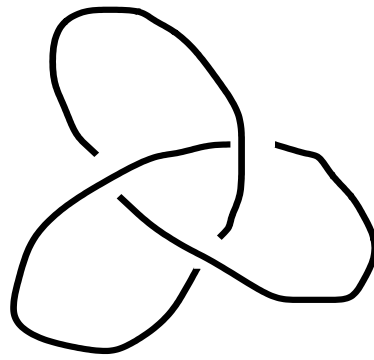
Knot K	$ \Delta_K(-1) $	$v_2(K)$
0	1	0
3_1	3	-12
4_1	5	12
5_1	5	-36
5_2	7	-24
$3_1\#3_1$	9	24
$3_1\#3_1\#3_1$	27	-36

Table 2: Fitting parameters $m_K(r)$, $C_K(r)$, $N_K(r)$ to the cylindrical self-avoiding polygons constructed by the dimerization method

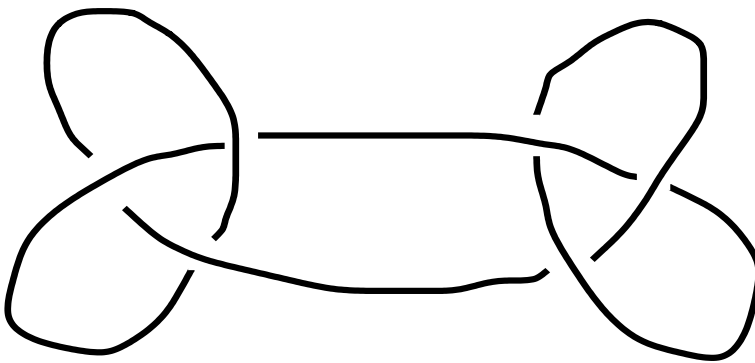
trivial	r=0.001	r=0.002	r=0.003	r=0.004	r=0.005	r=0.006	r=0.007
$C_K(r)$	1.055 ± 0.065	1.048 ± 0.006	1.066 ± 0.061	1.034 ± 0.060	1.001 ± 0.058	1.034 ± 0.057	1.024 ± 0.055
$N_K(r)$	278 ± 14	298 ± 15	315 ± 16	341 ± 17	377 ± 20	388 ± 20	417 ± 21
$m_K(r)$	-0.004 ± 0.034	-0.002 ± 0.03	0.0010 ± 0.031	-0.004 ± 0.030	-0.019 ± 0.028	0.001 ± 0.027	-0.006 ± 0.025
χ^2	3.0	2.7	1.2	2.1	2.0	2.2	1.7
3_1	r=0.001	r=0.002	r=0.003	r=0.004	r=0.005	r=0.006	r=0.007
$C_K(r)$	0.625 ± 0.021	0.638 ± 0.020	0.655 ± 0.061	0.669 ± 0.019	0.675 ± 0.020	0.687 ± 0.021	0.678 ± 0.020
$N_K(r)$	264 ± 21	280 ± 22	297 ± 24	314 ± 26	341 ± 30	375 ± 36	390 ± 38
$m_K(r)$	1.06 ± 0.10	1.091 ± 0.100	1.098 ± 0.097	1.128 ± 0.097	1.082 ± 0.095	1.048 ± 0.094	1.072 ± 0.095
χ^2	0.9	1.7	0.5	1.0	1.9	0.7	2.6
4_1	r=0.001	r=0.002	r=0.003	r=0.004	r=0.005	r=0.006	r=0.007
$C_K(r)$	0.124 ± 0.009	0.125 ± 0.009	0.125 ± 0.009	0.128 ± 0.012	0.125 ± 0.009	0.126 ± 0.009	0.131 ± 0.008
$N_K(r)$	236 ± 40	259 ± 47	286 ± 56	348 ± 75	348 ± 79	347 ± 79	334 ± 70
$m_K(r)$	1.269 ± 0.236	1.240 ± 0.244	1.176 ± 0.24	0.978 ± 0.218	1.118 ± 0.239	1.148 ± 0.243	1.247 ± 0.236
χ^2	2.6	2.3	1.0	2.0	1.7	2.3	1.4
5_1	r=0.001	r=0.002	r=0.003	r=0.004	r=0.005	r=0.006	r=0.007
$C_K(r)$	0.035 ± 0.006	0.041 ± 0.005	0.040 ± 0.005	0.037 ± 0.005	0.034 ± 0.007	0.036 ± 0.004	0.035 ± 0.005
$N_K(r)$	198 ± 56	246 ± 72	311 ± 116	265 ± 87	222 ± 62	326 ± 129	425 ± 222
$m_K(r)$	1.612 ± 0.486	1.335 ± 0.395	1.103 ± 0.428	1.380 ± 0.436	1.797 ± 0.452	1.306 ± 0.448	1.118 ± 0.473
χ^2	1.6	3.6	0.7	2.1	2.6	0.9	0.8
5_2	r=0.001	r=0.002	r=0.003	r=0.004	r=0.005	r=0.006	r=0.007
$C_K(r)$	0.068 ± 0.007	0.072 ± 0.007	0.068 ± 0.006	0.064 ± 0.006	0.060 ± 0.006	0.062 ± 0.006	0.061 ± 0.006
$N_K(r)$	226 ± 49	230 ± 51	283 ± 73	278 ± 73	322 ± 96	330 ± 101	290 ± 81
$m_K(r)$	1.401 ± 0.331	1.404 ± 0.340	1.234 ± 0.324	1.377 ± 0.347	1.317 ± 0.340	1.296 ± 0.348	1.418 ± 0.367
χ^2	1.3	2.0	1.2	1.6	2.0	1.3	1.0
$3_1\#3_1$	r=0.001	r=0.002	r=0.003	r=0.004	r=0.005	r=0.006	r=0.007
$C_K(r)$	0.166 ± 0.026	0.171 ± 0.029	0.161 ± 0.032	0.187 ± 0.032	0.184 ± 0.034	0.173 ± 0.038	0.161 ± 0.040
$N_K(r)$	259 ± 36	273 ± 41	278 ± 43	326 ± 57	318 ± 52	328 ± 58	325 ± 59
$m_K(r)$	2.150 ± 0.238	2.178 ± 0.248	2.311 ± 0.260	2.102 ± 0.251	2.225 ± 0.245	2.327 ± 0.266	2.448 ± 0.282
χ^2	1.9	0.9	1.4	1.9	2.0	1.1	1.6
$3_1\#3_1\#3_1$	r=0.001	r=0.002	r=0.003	r=0.004	r=0.005	r=0.006	r=0.007
$C_K(r)$	0.025 ± 0.020	0.023 ± 0.021	0.049 ± 0.038	0.021 ± 0.022	0.044 ± 0.039	0.030 ± 0.036	0.026 ± 0.029
$N_K(r)$	249 ± 77	244 ± 78	356 ± 152	260 ± 90	362 ± 163	330 ± 161	318 ± 138
$m_K(r)$	3.316 ± 0.689	3.443 ± 0.741	2.838 ± 0.672	3.602 ± 0.783	2.976 ± 0.719	3.358 ± 0.888	3.478 ± 0.804
χ^2	0.2	1.0	0.5	0.7	0.8	1.3	0.9



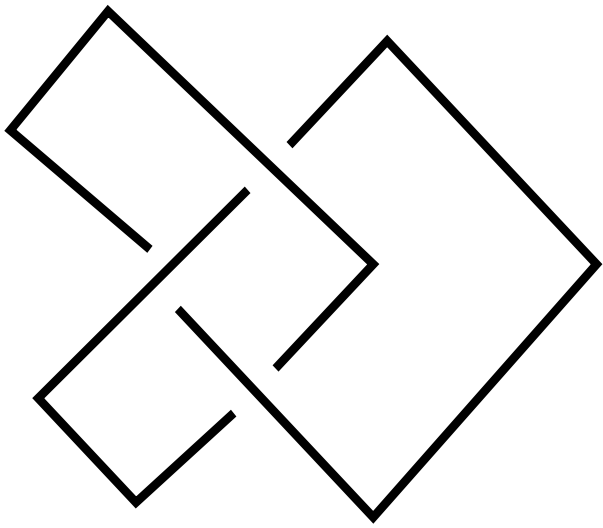
trivial knot



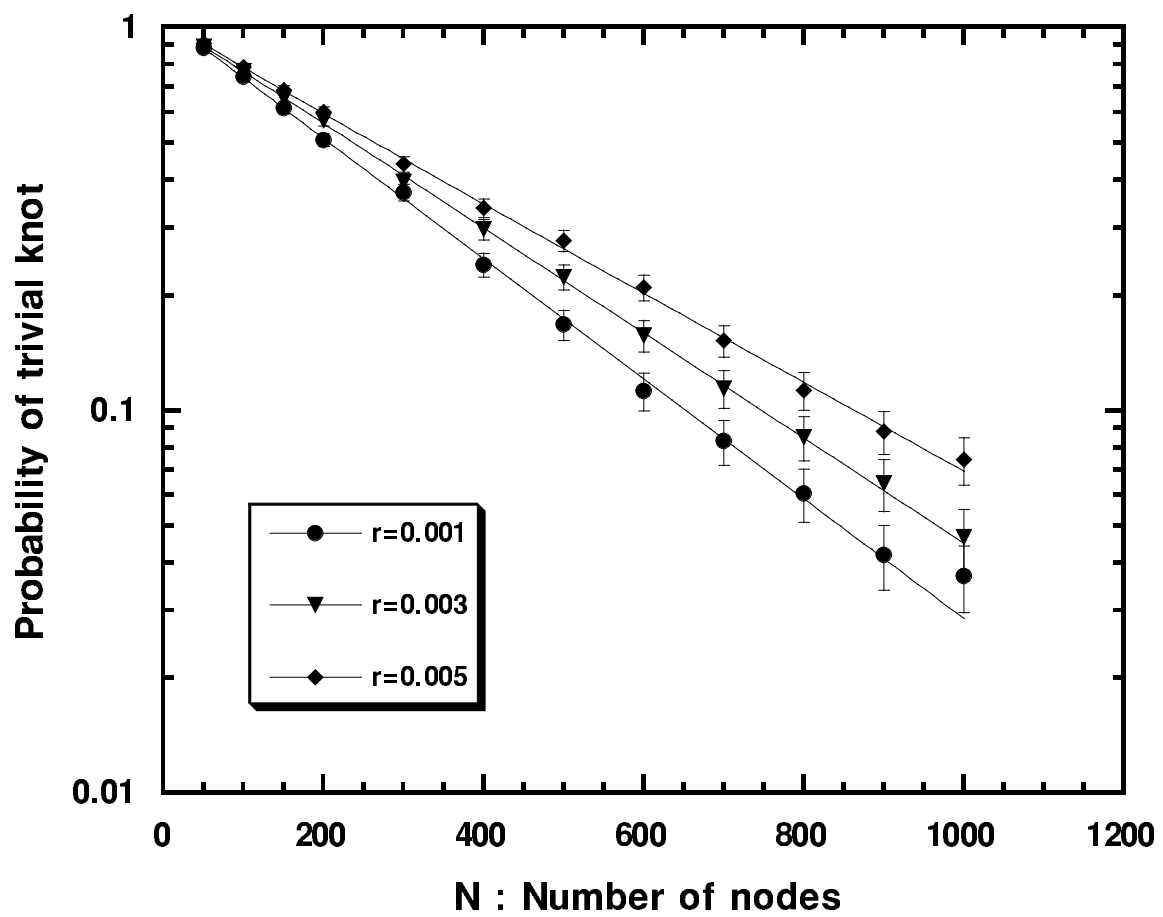
trefoil knot



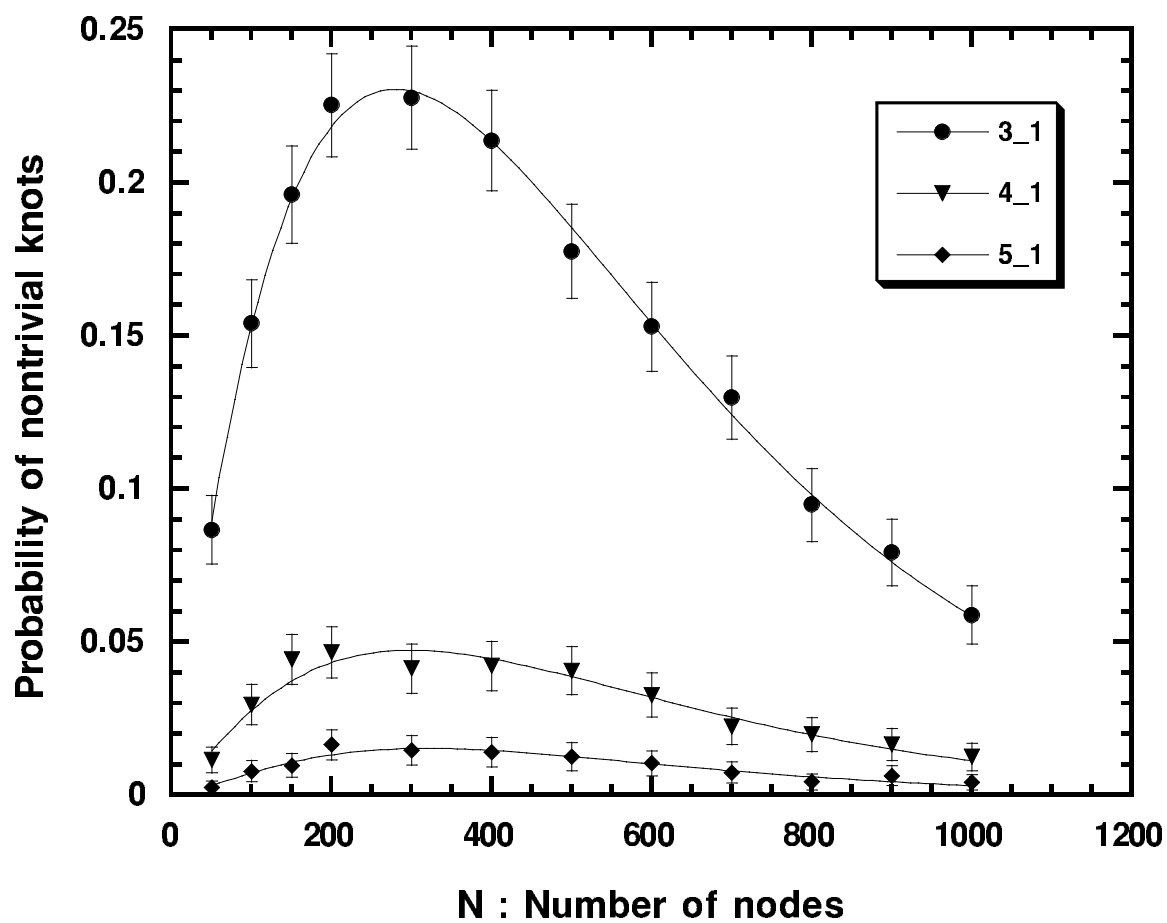
composit knot



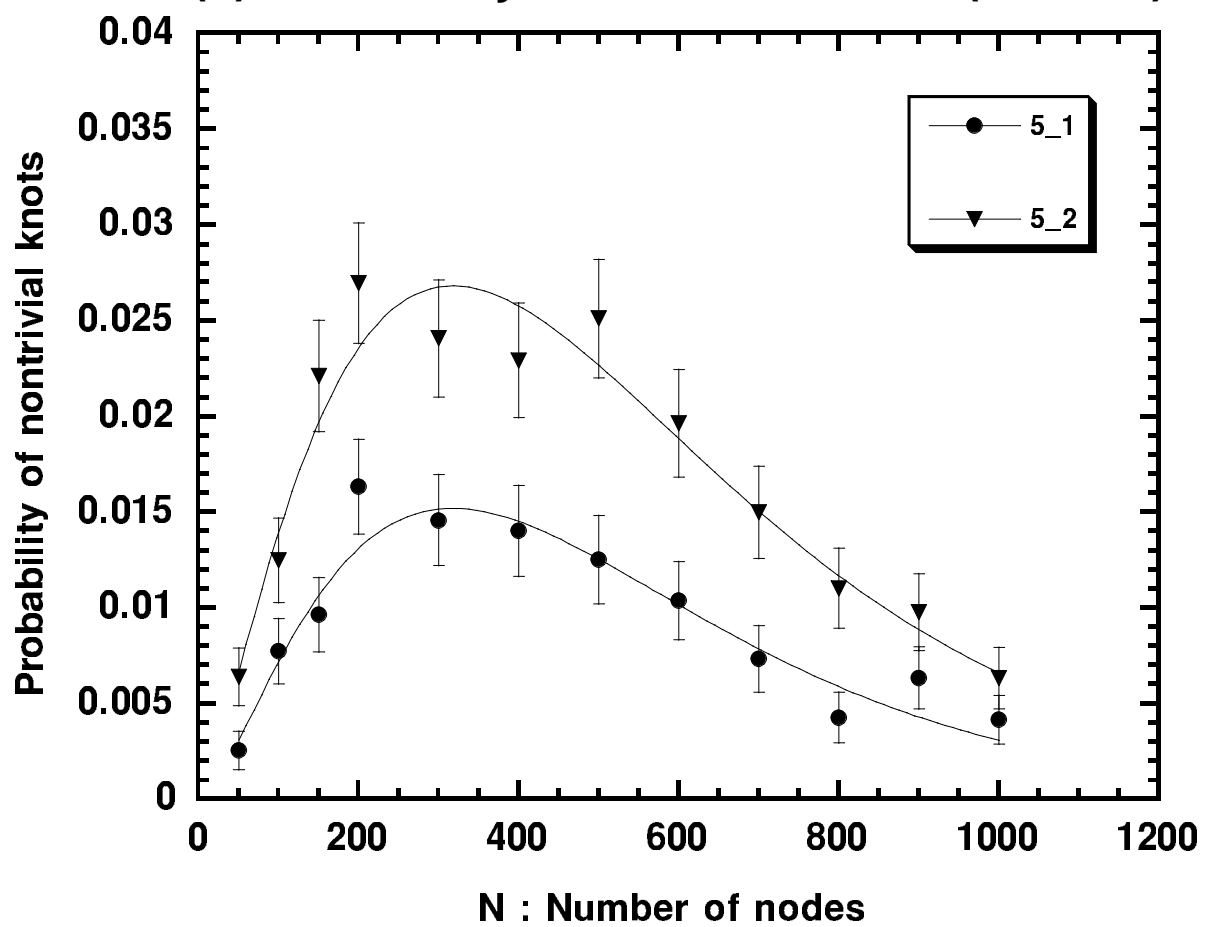
(a) Probability of trivial knot



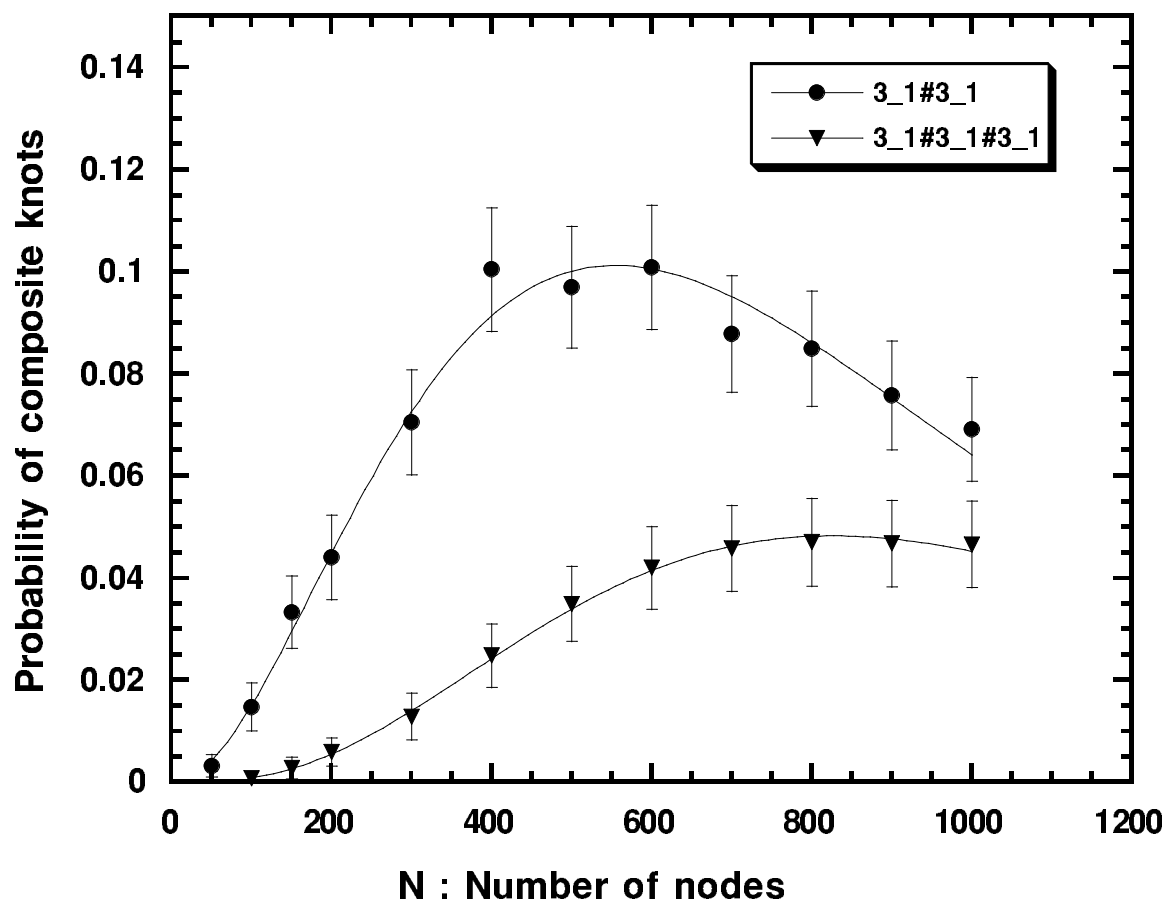
(a) Probability of nontrivial knots ($r=0.001$)

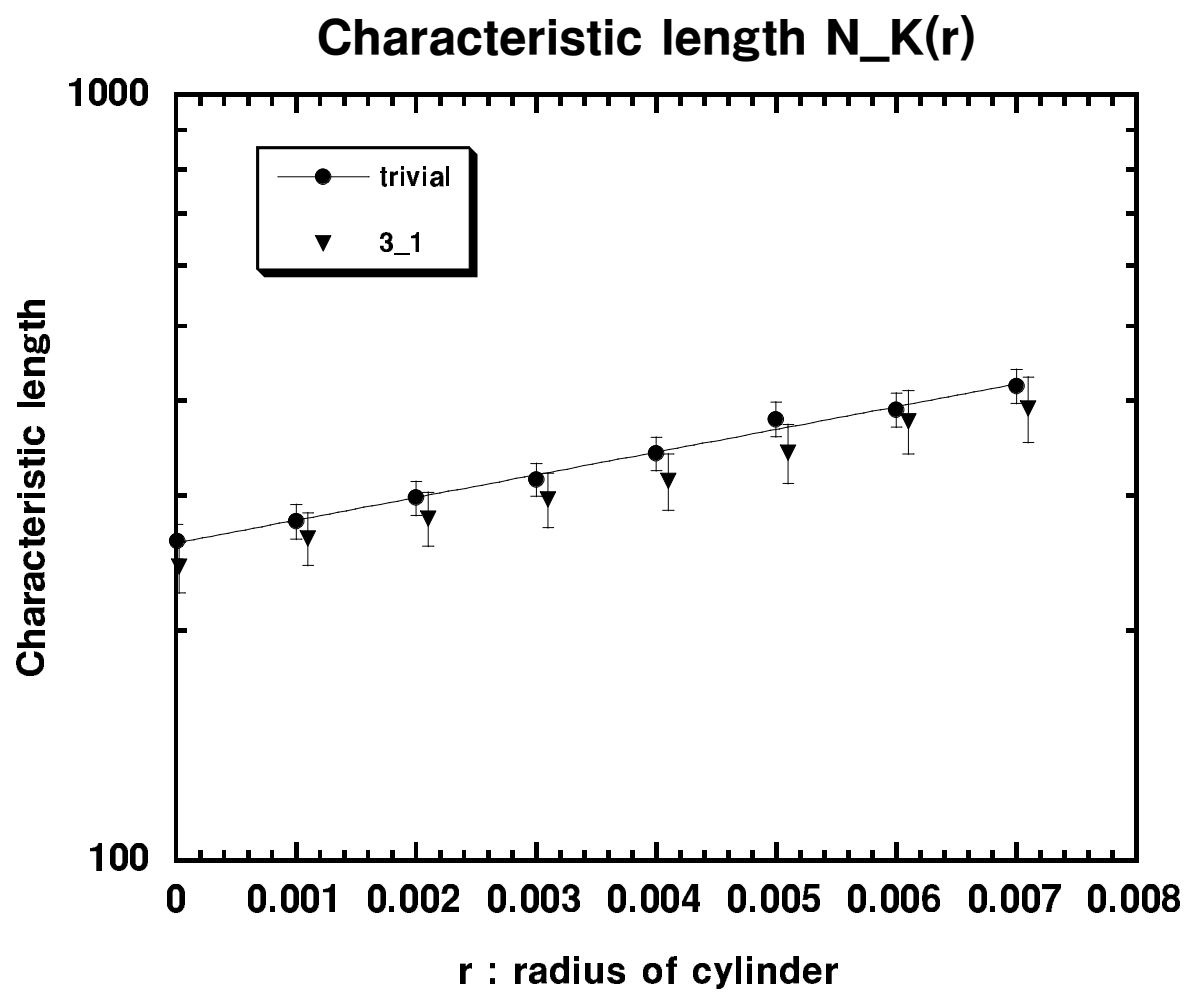


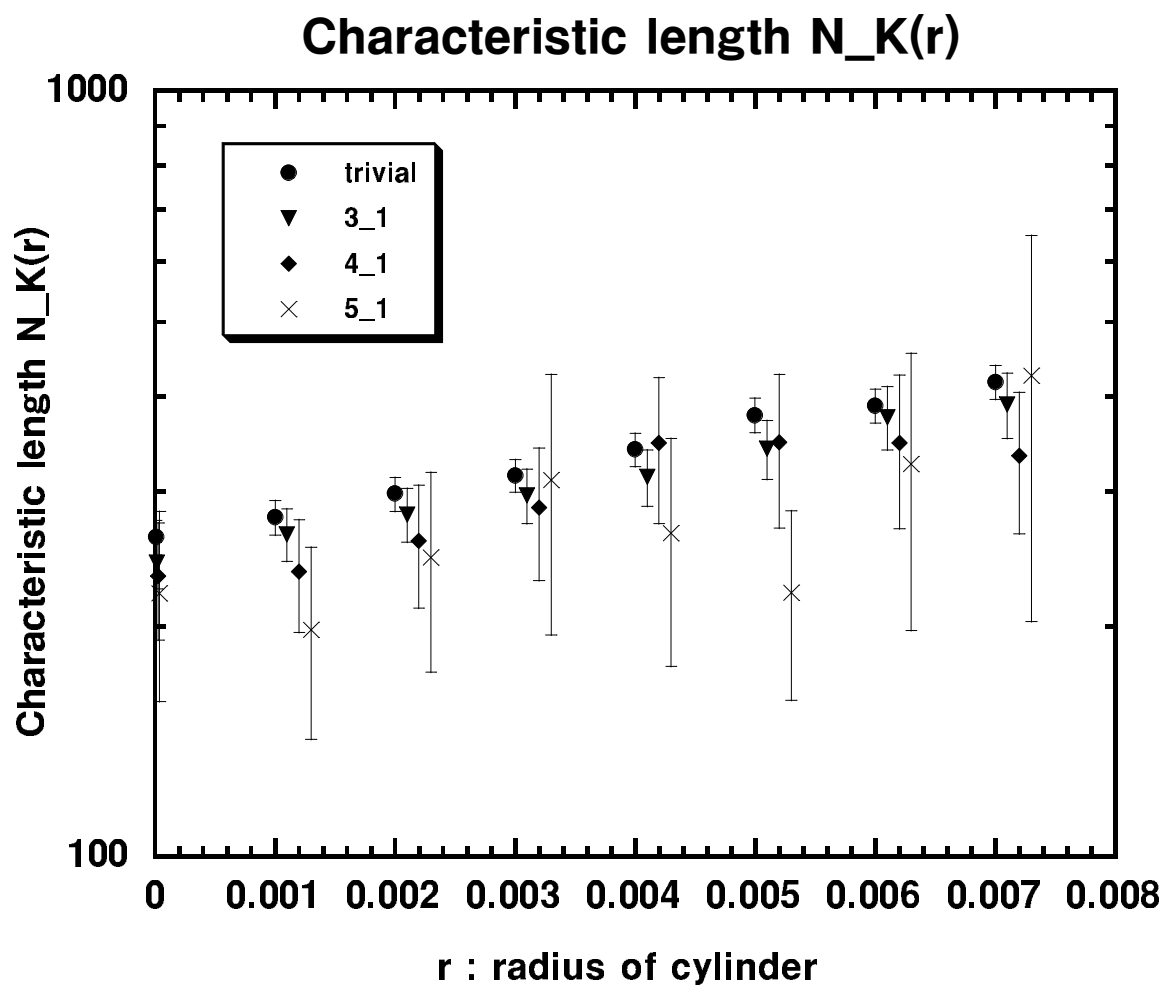
(a) Probability of nontrivial knot ($r=0.001$)

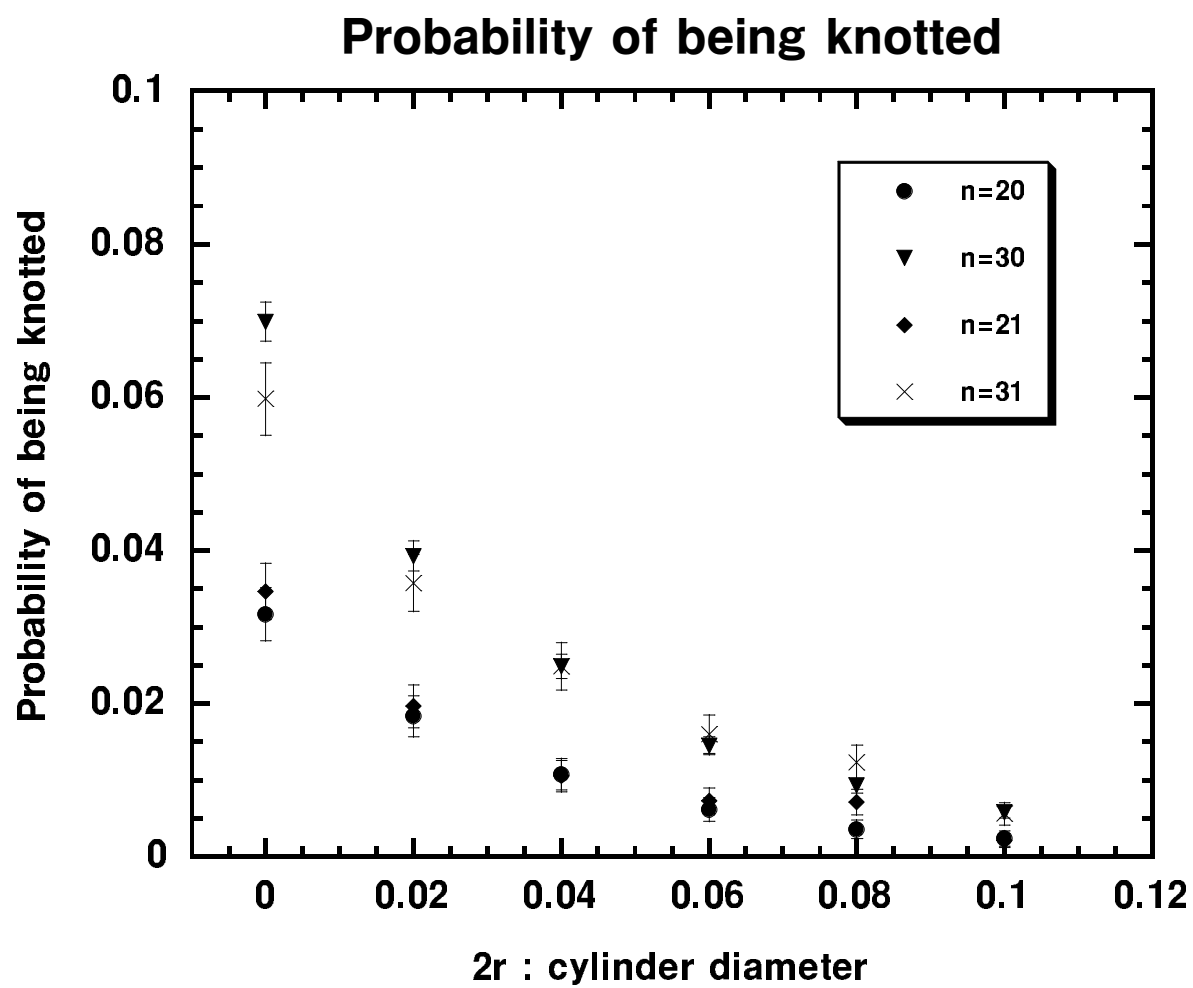


(a) Probability of composite knots ($r=0.001$)

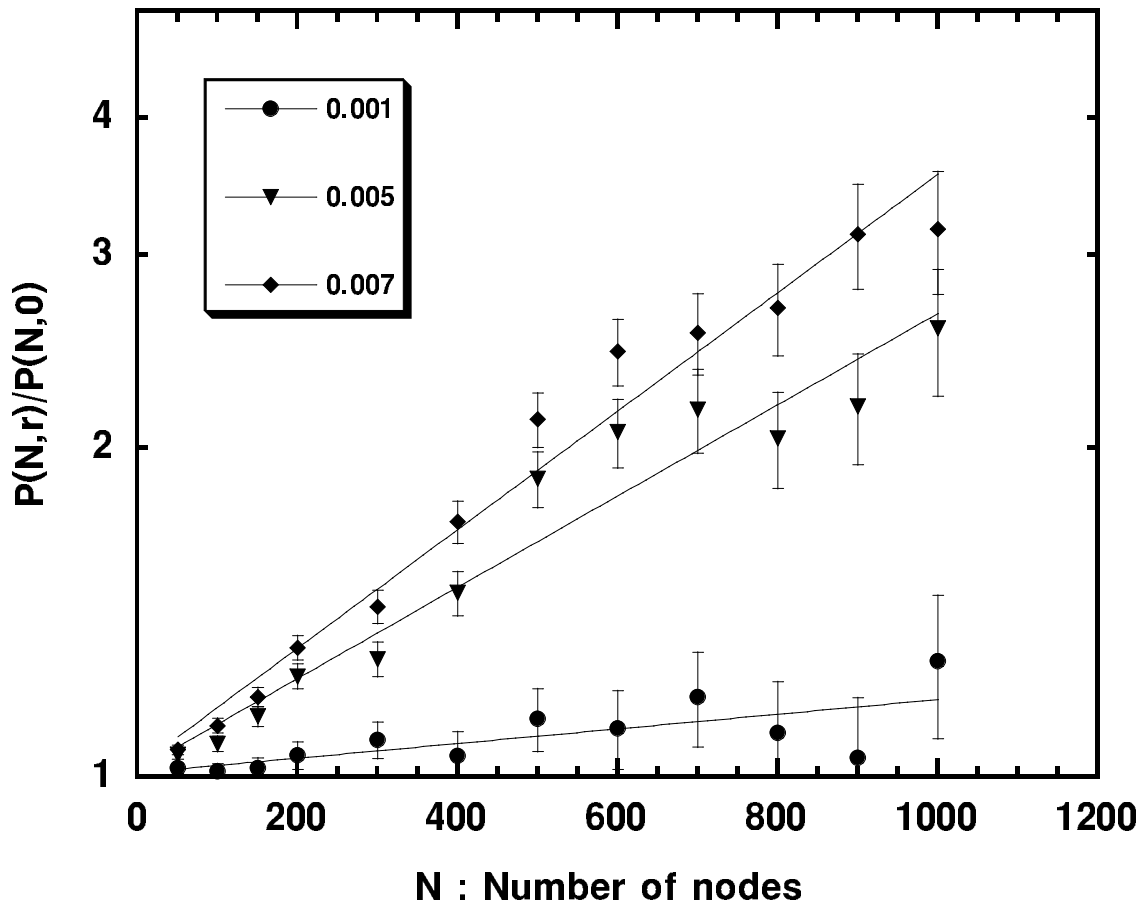








(a)trivial knot



(b) trefoil knot

